

Analyzing Multiple Nonlinear Time Series with Extended Granger Causality

Yonghong Chen

*Xi'an Jiaotong University, Xi'an 710049, P.R. China
Center for Complex Systems and Brain Sciences, Florida Atlantic University,
Boca Raton, FL 33431, USA*

Govindan Rangarajan

*Department of Mathematics and Centre for Theoretical Studies, Indian Institute of
Science, Bangalore 560 012, India
Jawaharlal Nehru Centre for Advanced Scientific Research, Bangalore, India*

Jianfeng Feng

*Department of Informatics, Sussex University, Brighton BN1 9QH, United
Kingdom*

Mingzhou Ding

*Center for Complex Systems and Brain Sciences, Florida Atlantic University,
Boca Raton, FL 33431, USA*

Abstract

Identifying causal relations among simultaneously acquired signals is an important problem in multivariate time series analysis. For linear stochastic systems Granger proposed a simple procedure called the Granger causality to detect such relations. In this work we consider nonlinear extensions of Granger's idea and refer to the result as Extended Granger Causality. A simple approach implementing the Extended Granger Causality is presented and applied to multiple chaotic time series and other types of nonlinear signals. In addition, for situations with three or more time series we propose a conditional Extended Granger Causality measure that enables us to determine whether the causal relation between two signals is direct or mediated by another process.

Key words: Granger Causality, Extended Granger Causality, nonlinear time series, vector autoregressive models, delay embedding reconstruction

Email addresses: ychen@walt.ccs.fau.edu (Yonghong Chen),
rangaraj@math.iisc.ernet.in (Govindan Rangarajan),
jianfeng@cogs.susx.ac.uk (Jianfeng Feng), ding@fau.edu (Mingzhou Ding).

1 Introduction

Given the deluge of multi-channel data generated by experiments in both science and engineering, the role of multivariate time series analysis, especially nonlinear time series processing, has become crucial in understanding the patterns of interaction among different elements of nonlinear systems. In particular, identifying causal relations among signals is important in fields ranging from physics to biology to economics. One approach to evaluating causal relations between two time series is to examine if the prediction of one series could be improved by incorporating information of the other. This was originally proposed by Wiener [1] and later formalized by Granger in the context of linear regression models of stochastic processes [2]. Specifically, if the variance of the prediction error of the second time series at the present time is reduced by inclusion of past measurements from the first time series in the linear regression model, then the first time series is said to have a causal influence on the second time series. The roles of the two time series can be reversed to address the question of causal influence in the opposite direction. From this definition it is clear that the flow of time plays a vital role in making direction related inference from time series data.

Since Granger causality was formulated for linear models, its direct application to nonlinear systems may or may not be appropriate, depending on the specific problem. In some cases, the linear Granger causality is able to identify the correct patterns of interaction for multiple nonlinear time series, but in some other cases, as will be shown later in this paper, it fails to do so. We deal with this issue by extending Granger's idea to nonlinear problems. Our starting point is the standard delay embedding reconstruction of the phase space attractors. Clearly, a full description of a given attractor requires a nonlinear set of equations. But, locally, one can approximate the dynamics linearly. Applying Granger's causality idea to each local neighborhood and averaging the resulting statistical quantity over the entire attractor results in Extended Granger Causality Index (EGCI). We examine the effectiveness of this idea on numerically generated nonlinear time series with known patterns of interaction.

Works related to the identification of interdependence in nonlinear systems have appeared in the literature [3,4,5,6,7]. Particularly relevant for the work in this paper are works based on delay coordinate embedding reconstruction of phase space. Along this direction a number of methods of detecting nonlinear interdependence or coupling based on nonlinear prediction theory have appeared in the past few years [8,9,10,11,12,13,14,15,16,17]. The basic ideas in these papers are similar, all involving the use of the points in a neighborhood in the reconstructed space to predict future dynamical behavior. In [9,10,11,12,13,14,15,16], time indices of neighborhood points in the space \mathbf{X}

reconstructed from one time series (x) are used to predict the dynamics in space \mathbf{Y} reconstructed from the second time series y . If this prediction is good enough, then it implies a dependence from x to y . Similarly, the reverse dependence can be found. Different authors define different criteria to quantify the goodness of the prediction, but the common assumption that nearby points in one reconstructed space \mathbf{X} map to nearby points in another reconstructed space \mathbf{Y} is adopted. These methods tend to detect strong interactions such as synchronization, phase synchronization or generalized synchronization. In order to detect weak interactions, a modification[17] was made by presenting a mixed-state prediction method where a reconstruction of mixing two time series was employed. It is important to note that all these nonlinear prediction based methods employ the same kind of predictor (a zeroth order predictor) which takes the mean or weighted mean as the prediction value. Since points in a given neighborhood come both from the past and the future of the reference point this kind of prediction does not account properly for the flow of time. Our idea differs from the previous methods in two main respects: (a) an linear regression predictor is employed for each local neighborhood and (b) as a consequence the flow of time is explicitly incorporated in the predictor which is an essential element of inferring causal relations in multiple time series [2]. A nonlinear approach that shares a number of similarities with ours has appeared in [5].

2 Theory

In this section we will first review the basic idea of Granger Causality formulated for analyzing linear systems and then propose a generalization of Granger's idea to attractors reconstructed with delay coordinates.

Granger Causality: The method of detecting causal relations among multiple linear time series is based on linear prediction theory. For a stationary time series $x(t)$, consider the following AutoRegressive (AR) prediction of the current value of $x(t)$ based on m past measurements:

$$x(t) = \sum_{j=1}^m \alpha_j x(t-j) + \varepsilon_x(t). \quad (1)$$

Here $\varepsilon_x(t)$ is the prediction error whose magnitude can be evaluated by its variance $var(\varepsilon_x(t))$. Suppose that simultaneously we have also acquired another stationary time series $y(t)$. Consider the following prediction of the current

value of $x(t)$ based both on its own past values and the past values of $y(t)$:

$$x(t) = \sum_{j=1}^m a_j x(t-j) + \sum_{j=1}^m b_j y(t-j) + \varepsilon_{x|y}(t). \quad (2)$$

If the prediction improves by incorporating the past values of $y(t)$, that is, $\text{var}(\varepsilon_{x|y}(t)) < \text{var}(\varepsilon_x(t))$ in some suitable sense, then we say that $y(t)$ has a causal influence on $x(t)$. Similarly, we may consider

$$y(t) = \sum_{j=1}^m \beta_j y(t-j) + \varepsilon_y(t), \quad (3)$$

$$y(t) = \sum_{j=1}^m c_j x(t-j) + \sum_{j=1}^m d_j y(t-j) + \varepsilon_{y|x}(t). \quad (4)$$

and say that $x(t)$ has a causal influence on $y(t)$ if $\text{var}(\varepsilon_{y|x}(t)) < \text{var}(\varepsilon_y(t))$. We note that Eqs. (2) and (4) together form the following Vector AutoRegressive model (VAR):

$$\begin{aligned} x(t) &= \sum_{j=1}^m a_j x(t-j) + \sum_{j=1}^m b_j y(t-j) + \varepsilon_{x|y}(t), \\ y(t) &= \sum_{j=1}^m c_j x(t-j) + \sum_{j=1}^m d_j y(t-j) + \varepsilon_{y|x}(t), \end{aligned} \quad (5)$$

where standard techniques exist to estimate such models from time series data.

Extended Granger Causality: Consider two nonlinear time series $x(t)$ and $y(t)$. The joint dynamics is reconstructed with the following delay vector [18,19]

$$\mathbf{z}(t) = (\mathbf{x}(t)^T, \mathbf{y}(t)^T)^T, \quad (6)$$

where $\mathbf{x}(t) = (x(t), x(t - \tau_1), \dots, x(t - (m_1 - 1)\tau_1))^T$, $\mathbf{y}(t) = (y(t), y(t - \tau_2), \dots, y(t - (m_2 - 1)\tau_2))^T$, m_i is embedding dimension and τ_i is time delay for $i = 1, 2$. Usually, the embedding dimensions and time delays for different series can be different. However when we investigate Granger causality, the time delays must be equal so that causal inferences can be made. Hereafter we take $\tau_1 = \tau_2 = \tau$.

In the delay embedding space, there exists a function \mathbf{f} that maps a given point $\mathbf{z}(t)$ to its observed image $\mathbf{z}(t + \tau)$. Usually, this function has no known analytical form but can be locally approximated by a linear map around some reference point [20,21]: $\mathbf{z}(t + \tau) = \mathbf{A}\mathbf{z}(t) + \mathbf{r}(t)$, where \mathbf{A} is $(m_1 + m_2) \times (m_1 + m_2)$

coefficient matrix which can be determined by the least-squares technique and $\mathbf{r}(t)$ is the error vector. Substituting Eq.(6) in the above relations, we get the following equations:

$$\begin{aligned} \begin{pmatrix} x(t + \tau) \\ y(t + \tau) \end{pmatrix} &= \mathbf{A}_1 \begin{pmatrix} x(t) \\ y(t) \end{pmatrix} + \mathbf{A}_2 \begin{pmatrix} x(t - \tau) \\ y(t - \tau) \end{pmatrix} + \\ &\dots + \mathbf{A}_m \begin{pmatrix} x(t - (m - 1)\tau) \\ y(t - (m - 1)\tau) \end{pmatrix} + \begin{pmatrix} \varepsilon_{x|y} \\ \varepsilon_{y|x} \end{pmatrix}, \end{aligned} \quad (7)$$

where $\mathbf{A}_i = \begin{pmatrix} a_{11}^{(i)} & a_{12}^{(i)} \\ a_{21}^{(i)} & a_{22}^{(i)} \end{pmatrix}$, $\varepsilon_{x|y}$ and $\varepsilon_{y|x}$ are the error terms, and we have assumed $m_1 = m_2 = m$ for simplicity. If $m_1 \neq m_2$, some diagonal terms of \mathbf{A}_i would turn out to be zero.

We note that Eq. (7) is just another form of Eq. (5) for non-unit time step. Therefore, in Eq. (7), $\varepsilon_{x|y}$ (or $\varepsilon_{y|x}$) actually gives the prediction error of x (or y) after incorporating y (or x). To proceed further, we also reconstruct each series independently around the x and y parts of the same reference point using linear regression approximations to obtain

$$\begin{aligned} x(t + \tau) &= \sum_{j=1}^{m_1} \alpha_j x[t + (j - 1)\tau] + \varepsilon_x, \\ y(t + \tau) &= \sum_{j=1}^{m_2} \beta_j y[t + (j - 1)\tau] + \varepsilon_y. \end{aligned} \quad (8)$$

We can now apply the ideas from Granger causality to these local linear systems. Thus, if the ratio of the errors $\frac{\text{var}(\varepsilon_{x|y})}{\text{var}(\varepsilon_x)}$ (or $\frac{\text{var}(\varepsilon_{y|x})}{\text{var}(\varepsilon_y)}$) is less than 1, it implies y (or x) has causal influence on x (or y). So far, this procedure only involves data in one local neighborhood around a given reference point. Clearly, for nonlinear systems the coefficient matrix in the linear approximation is a function of the local neighborhood. We repeat the process above for a set of chosen neighborhoods scattered over the entire attractor and average the error ratios from all the neighborhoods to obtain the Extended Granger Causality. See below for a more formal formulation.

The idea above is actually very similar to other ideas of detecting directional interdependence based on nonlinear mutual prediction [9,10,11,12,14,15,16,17]. The difference is that the previous work used the average or weighted average value of the images of the points in a given neighbor as the basis for predic-

tion. Thus they suffer from the lacuna that points in the neighborhood of the reference point have no explicit time relations to the reference point itself. On the other hand, we employ a linear model which preserves explicit time relations and are therefore able to derive unambiguous causality relationships.

Summarizing, we propose the following four-step procedure to evaluate causal relations between two nonlinear time series:

- (1) Reconstruct the attractor using the delay coordinate embedding technique [cf. Eq. (6)].
- (2) Fit an autoregressive model for all the points in the neighborhood Θ of a reference point \mathbf{z}_0 in the reconstructed space $\mathbf{R}^{m_1+m_2}$, where $\Theta = \{\mathbf{z} : |\mathbf{z} - \mathbf{z}_0| \leq \delta\}$.
- (3) Perform the reconstruction and fitting process on the individual x and y time series in the same neighborhood and compute the error ratio defined earlier. Average the error ratio over a number of local neighborhoods in order to sample the full attractor adequately. Compute the Extended Granger Causality Index (EGCI) defined as $\Delta_{y \rightarrow x} = \langle 1 - \frac{\text{var}(\varepsilon_{x|y})}{\text{var}(\varepsilon_x)} \rangle$, where $\langle \cdot \rangle$ stands for averaging over the neighborhood sampling the entire attractor.
- (4) Compute EGCI as a function of the neighborhood size δ . For linear systems this index will stay roughly the same as δ becomes smaller. For nonlinear systems this index, in the small δ limit, reveals the true nonlinear causal relation which may or may not be captured at the full attractor level (i.e. taking δ to be the size of the whole attractor).

To reconstruct the attractor, the embedding dimension and time delay have to be determined. Usually the embedding dimension is determined by the false nearest neighbor technique [22] and the time delay is obtained as the first minimum of the mutual information function [23]. If the reconstructed attractor is a fixed point with some noise, then a criterion such as AIC [24] for linear stochastic processes can be used to determine the order of the model. A difficult issue for the present work is to determine the optimal neighborhood size δ . The number of points in the neighborhood should be large enough to establish good statistics. On the other hand, the size of the neighborhood should be small enough so that linearization is valid. In step (4) above we seek a compromise by examining the EGCI as a function of δ in the attempt to get to the true nonlinear effect when δ becomes small enough. We refer to this step as a zooming-in procedure. For sufficiently large dataset, the usual rule is that, the smaller the neighborhood size, the better the nonlinear prediction achieved [14,15,17].

Conditional Extended Granger Causality: The above analysis for two time series can be extended to more than two time series by analyzing them pairwise.

However, pairwise analysis of more than two time series cannot detect indirect causal influences, an issue that has been addressed in linear time series analysis [25]. For example, consider three time series A, B and C. Two possible causal relations among them are shown in Figures 1(a) and (b). In Figure 1(a), the causal influence or driving from A to C is indirect and mediated by B. In Figure 1(b), both direct and indirect influences exist. Pairwise analysis would show an arrow from A to C and thus cannot separate these two cases. We propose the following procedure for the case of three time series which, as we show in the next section, is able to reveal the true patterns of causal interactions.

Suppose $s_A(t), s_B(t), s_C(t)$ are the given three time series, we reconstruct vector \mathbf{z} in whole space as[19]:

$$\mathbf{z}(t) = (\mathbf{s}_A(t)^T, \mathbf{s}_B(t)^T, \mathbf{s}_C(t)^T)^T, \quad (9)$$

where $\mathbf{s}_A(t) = (s_A(t), s_A(t-\tau), \dots, s_A(t-(m_1-1)\tau))^T$, $\mathbf{s}_B(t) = (s_B(t), s_B(t-\tau), \dots, s_B(t-(m_2-1)\tau))^T$, $\mathbf{s}_C(t) = (s_C(t), s_C(t-\tau), \dots, s_C(t-(m_3-1)\tau))^T$. Then the vector autoregression obtained from a local linear approximation is given by

$$\begin{aligned} s_A(t+\tau) &= \sum_{i=1}^{m_1} a_{11}^{(i)} s_A[t-(i-1)\tau] + \sum_{i=1}^{m_2} a_{12}^{(i)} s_B[t-(i-1)\tau] \\ &\quad + \sum_{i=1}^{m_3} a_{13}^{(i)} s_C[t-(i-1)\tau] + \varepsilon_{A|BC}, \\ s_B(t+\tau) &= \sum_{i=1}^{m_1} a_{21}^{(i)} s_A[t-(i-1)\tau] + \sum_{i=1}^{m_2} a_{22}^{(i)} s_B[t-(i-1)\tau] \\ &\quad + \sum_{i=1}^{m_3} a_{23}^{(i)} s_C[t-(i-1)\tau] + \varepsilon_{B|AC}, \\ s_C(t+\tau) &= \sum_{i=1}^{m_1} a_{31}^{(i)} s_A[t-(i-1)\tau] + \sum_{i=1}^{m_2} a_{32}^{(i)} s_B[t-(i-1)\tau] \\ &\quad + \sum_{i=1}^{m_3} a_{33}^{(i)} s_C[t-(i-1)\tau] + \varepsilon_{C|AB}. \end{aligned} \quad (10)$$

The term $\varepsilon_{C|AB}$ is the prediction error of the series \mathbf{s}_C after incorporating both \mathbf{s}_A and \mathbf{s}_B . If this prediction is no better than the prediction obtained by incorporating only the series \mathbf{s}_B , it means \mathbf{s}_A has no direct causal influence on \mathbf{s}_C . Therefore we can define a Conditional Extended Granger Causality Index (CEGCI) as $\Delta_{A \rightarrow C|B} = \langle 1 - \frac{\text{var}(\varepsilon_{C|AB})}{\text{var}(\varepsilon_{C|B})} \rangle$. This can be used to distinguish between direct and indirect causal relations. Conditional causality

indices between other time series pairs can be similarly defined.

It is worth mentioning that for more than three time series, if the causality between any two time series is indirect, then taking one additional series or more than one additional series in the causality chain as the conditional one(s) will not make the results any different. Therefore analysis of three time series is sufficient to detect the intrinsic causal influences in any multiple time series system.

3 Numerical Simulations and Discussion

In order to make the whole discussion concrete, we study some examples. The number of reference points around the attractor is 100 for all the examples.

Example 1: Let's consider two time series generated from unidirectionally coupled 2D maps. Two different coupling schemes, one linear and one nonlinear, are examined. The system with linear coupling is written as

$$\begin{aligned} x(n) &= 3.4x(n-1)(1-x^2(n-1))e^{-x^2(n-1)} + 0.8x(n-2), \\ y(n) &= 3.4y(n-1)(1-y^2(n-1))e^{-y^2(n-1)} + 0.5y(n-2) + cx(n-2), \end{aligned} \quad (11)$$

and the system with nonlinear coupling is

$$\begin{aligned} x(n) &= 3.4x(n-1)(1-x^2(n-1))e^{-x^2(n-1)} + 0.8x(n-2), \\ y(n) &= 3.4y(n-1)(1-y^2(n-1))e^{-y^2(n-1)} + 0.5y(n-2) + cx^2(n-2). \end{aligned} \quad (12)$$

It is obvious that y is driven by x in both systems. In order to make the simulations realistic, some system noise and measurement noise are added to the time series. The attractor reconstructed from the x time series is given in Figure 2(a). Figures 2(b) and 2(c) give the reconstructed attractors from the y time series driven linearly and nonlinearly by x with the coupling strength $c = 0.5$.

Both these cases are analyzed using our procedure in the previous section with $m = 2$ and $\tau = 1$. We obtain the EGCI as a function of the neighborhood size δ in Figure 3. For both linear driving [Fig. 3(a)] and nonlinear driving [Fig. 3(b)], $\Delta_{y \rightarrow x}$ (shown as the thicker curve) is seen to be zero. Thus x is not influenced by y as expected from the construction of our model. In Fig. 3(a), $\Delta_{x \rightarrow y}$ is non-zero starting from large neighborhood sizes δ and increases as δ decreases. This implies that x has a causal influence on or drives y . Further,

since $\Delta_{x \rightarrow y}$ is non-zero even for large δ values, this means that even a linear causality analysis would have detected the correct causal relations in this case. On the other hand, in Figure 3(b) (for nonlinear driving), $\Delta_{x \rightarrow y}$ becomes non-zero only when δ is sufficiently small. In this case, a linear causality analysis would fail to detect the correct pattern of driving. This example illustrates the importance of nonlinear causality analysis in such cases.

Example 2: We consider two time series generated by two coupled two-dimensional ODEs where the fixed point in the origin is stable:

$$\begin{aligned}
 \dot{x}_1 &= -0.25x_1 + x_2 - x_2^3, \\
 \dot{x}_2 &= x_1 - x_2 - x_1x_2, \\
 \dot{y}_1 &= -0.25y_1 + y_2 - y_2^3 + cx_1^2, \\
 \dot{y}_2 &= y_1 - y_2 - y_1y_2.
 \end{aligned} \tag{13}$$

Adding some system noise and measurement noise and taking x_1 and y_1 as the acquired signals, we get two modified time series x and y . Clearly in this case x series drives y series. Reconstructing the attractors from these two time series with $\tau = 2$, finding the neighborhood of every reference point and fitting a second order AR model ($m = 2$) in every neighborhood, we obtain the Extended Granger Causality Index (EGCI) as a function of the neighborhood size δ for different coupling strengths as shown in Figure 4(a). We make three observations. First, $\Delta_{y \rightarrow x} \approx 0$, whereas $\Delta_{x \rightarrow y}$ is non-zero, clearly demonstrating that the x series drives the y series but not vice-versa. Second, the level of EGCI is proportional to the coupling strength. Third, since the processes here are linear, the EGCI is not a function of δ .

Example 3: Next we look at an ODE system exhibiting chaotic behaviors. The following two coupled Rössler oscillators are considered:

$$\begin{aligned}
 \dot{x}_1 &= -(y_1 + z_1), \\
 \dot{y}_1 &= x_1 + 0.2y_1, \\
 \dot{z}_1 &= 0.2 + z_1(x_1 - 4.7). \\
 \dot{x}_2 &= -(y_2 + z_2) + cx_1, \\
 \dot{y}_2 &= x_2 + 0.2y_2, \\
 \dot{z}_2 &= 0.2 + z_2(x_2 - 4.7).
 \end{aligned} \tag{14}$$

As done earlier, some system noise and measurement noise are added to the two time series x_1 and x_2 to obtain x and y time series. Reconstructing the attractors with $m = 3$ and $\tau = 2$ and fitting linear models in every local neighborhood, we obtain EGCI shown in Figure 4(b). It is seen that x has a causal influence on y as expected. Besides, $\Delta_{x \rightarrow y}$ is non-zero even for large

neighborhood sizes. Thus, a linear causality analysis would detect the correct causal relations in this strongly nonlinear system.

Example 4: To show how to distinguish the pattern of interaction shown in Figure 1(b) from that shown in Figure 1(a), let us consider three time series. Both linear systems and nonlinear systems are considered.

For a linear stochastic system the following three coupled AR(1) models are considered:

$$\begin{aligned} x(n) &= 0.2x(n-1) + \varepsilon_1, \\ y(n) &= 0.5y(n-1) + 0.5x(n-1) + \varepsilon_2, \\ z(n) &= 0.4z(n-1) + 0.3y(n-1) + cx(n-1) + \varepsilon_3. \end{aligned} \tag{15}$$

For chaotic time series, the following three coupled 1-d maps are considered:

$$\begin{aligned} x(n) &= 3.4x(n-1)(1-x^2(n-1))e^{-x^2(n-1)}, \\ y(n) &= 3.4y(n-1)(1-y^2(n-1))e^{-y^2(n-1)} + 0.5x(n-1), \\ z(n) &= 3.4z(n-1)(1-z^2(n-1))e^{-z^2(n-1)} + 0.3y(n-1) + cx(n-1). \end{aligned} \tag{16}$$

Here x , y and z correspond to A, B and C in Figure 1. In addition, $c = 0$ simulates the indirect causality case (Fig. 1(a)) and $c = 0.5$ simulates the direct causality case (Fig. 1(b)).

Numerical results for the linear case are shown in Figure 5 and results for the chaotic time series are shown in Figure 6. Figures 5(a) and 6(a) display results obtained using pairwise analysis. Similar plots are obtained for both $c = 0$ and $c = 0.5$. As we can see, based on just pairwise analysis, one would conclude that Figure 1(b) is the pattern of interaction for both $c = 0$ and $c = 0.5$. That is, the direct and indirect causal relationships cannot be separated by pairwise analysis alone. Figures 5(b) and 6(b) give the results obtained by simultaneously analyzing all three time series using conditional EGCI. In this case, for $c = 0$ we obtain $\Delta_{x \rightarrow z|y} \approx 0$ (solid curve) indicating that no direct causal relation exists between x and z . Thus the correct causality graph [Figure 1(a)] is obtained. On the other hand, for $c = 0.5$, $\Delta_{x \rightarrow z|y}$ is non-zero (dotted curve) indicating direct causality between x and z and the causality graph shown in Figure 1(b) is obtained.

4 Conclusions

We have extended the Granger causality theory to nonlinear time series by incorporating the embedding reconstruction technique for multivariate time series. A four-step algorithm was presented and used to analyze various linear and nonlinear coupled systems. The following conclusions were found:

- (1) Linear Granger causality analysis may or may not work for nonlinear time series. On the other hand, our method of applying the Extended Granger Causality Index to nonlinear time series always gives reliable results.
- (2) When three or more time series have to be analyzed, the Conditional Extended Granger Causality Index proposed here can distinguish between direct and indirect causal relationships between any two of the time series. This is not possible using simple pairwise analysis.

As with other methods for analyzing nonlinear time series, the amount of data required for reliable analysis can be large. Possible improvements along this direction are being studied.

Acknowledgments

The work was supported by ONR, NSF and NIMH. GR is also supported by DRDO, India and the Homi Bhabha Fellowship.

References

- [1] N. Wiener (1956). The theory of prediction. In: E. F. Beckenbach (Ed) Modern Mathematics for Engineers, Chap 8. McGraw-Hill, New York.
- [2] C. W. J. Granger (1969). Investigating causal relations by econometric models and cross-spectral methods, *Econometrica*, *37*, 424-438.
- [3] M. B. Priestley (1988). *Nonlinear and Non-stationary Time Series Analysis*, Academic Press.
- [4] F. Wendling, F. Bartolomei, J. Bellanger, P. Chauvel (2001). Interpretation of interdependencies in epileptic signals using a macroscopic physiological model of the EEG, *Clin. Neurophysiol.*, *112*, 1201-1218.
- [5] W. A. Freiwald, P. Valdes, J. Bosch et. al. (1999). Testing non-linearity and directedness of interactions between neural groups in the macaque inferotemporal cortex, *J. Neuroscience Methods*, *94*, 105-119.
- [6] T. Schreiber (2000). Measuring information transfer, *Phys. Rev. Lett.*, *85*, 461-464.
- [7] O. Sakata, T. Shiina, and Y. Saito (2002). Multidimensional directed information and its application, *Electronics and Commun. in Japan, part 3*, *85*, 45-55.
- [8] H. Kantz and T. Schreiber (1997) *Nonlinear Time series Analysis*, Cambridge University Press.
- [9] J. Arnhold, P. Grassberger, K. Lehnertz and C. E. Elger (1999). A robust method for detecting interdependences: application to intracranially recorded EEG, *Physica D*, *134*, 419-430.
- [10] R. Quian Quiroga, J. Arnhold and P. Grassberger (2000). Learning drive-response relationships from synchronization patterns, *Phys. Rev. E*, *61*, 5142-5148.
- [11] R. Quian Quiroga, A. Kraskov, T. Kreuz and P. Grassberger (2002). Performance of different synchronization measures in real data: A case study on electroencephalographic signals, *Phys. Rev. E*, *65*, 041903.
- [12] M. Quyen, J. Martinerie, C. Adam and F. Varela J. (1999). Nonlinear analyses of interictal EEG map the brain interdependences in human focal epilepsy, *Physica D*, *127*, 250-266.
- [13] J. Bhattacharya, E. Pereda and H. Petsche (2003) Effective detection of coupling in short and noisy bivariate data, *IEEE Trans. Systems, Man, and Cybernetics Part B* *33*, 85-95.
- [14] M. Breakpear, J. R. Terry, (2002). Detection and description of non-linear interdependence in normal multichannel human EEG data, *Clin. Neurophysiol.*, *113*, 735-753.

- [15] M. Breakpear, J. R. Terry, (2002). Topographic organization of nonlinear interdependence in multichannel human EEG, *NeuroImage*, 16, 822-835.
- [16] S.J. Schiff, P. So, T. Chang, R. E. Burke and T. Sauer (1996). Detecting dynamical interdependence and generalized synchrony through mutual prediction in a neural ensemble, *Phys. Rev. E*, 54, 6708.
- [17] M. Wiesenfeldt, U. Parlitz and W. Lauterborn (2001). Mixed state analysis of multivariate time series, *Intl. J. Bifurcation and Chaos*, 11, 2217-2226.
- [18] M. Casdagli (1992). A dynamical systems approach to modeling input-out systems, In: *Nonlinear Modeling and Forecasting*, Proc. Vol. XII (Ed.) M. Casdagli and S. Eubank, Addison-Wesley, 265-281.
- [19] S. Boccaletti, D. L. Valladares, L. M. Pecora, et al, (2002). Reconstructing embedding spaces of coupled dynamical systems from multivariate data, *Phys. Rev. E* 65, 035204.
- [20] J.-P. Eckmann and D. Ruelle (1985). Ergodic theory of chaos and strange attractors, *Rev. Mod. Phys.* 57, 617-656.
- [21] J. D. Farmer and J. J. Sidorowich (1987). Predicting chaotic time series, *Phys. Rev. Lett.* 59, 845-848.
- [22] M. B. Kennel, R. Brown and H. D. Abarbanel (1992). Determining minimum embedding dimension using a geometrical construction, *Phys. Rev. A* 45, 3403-3411.
- [23] A. M. Fraser and H. L. Swinney(1986). Independent coordinates for strange attractors from mutual information, *Phys. Rev. A* 33, 1134-1140.
- [24] H. Lütkepohl, (1993) *Introduction to Multiple Time Series Analysis*, Springer-Verlag.
- [25] M. Kaminski, M. Ding, W.A. Truccolo and S.L. Bressler (2001). Evaluating causal relations in neural systems: Granger causality, directed transfer function and statistical assessment of significance, *Biol. Cybern.* 85, 145-157.

Figure Caption

Figure 1: Two patterns of causal interactions. (a) A drives C by way of B and (b) There is a direct pathway from A to C.

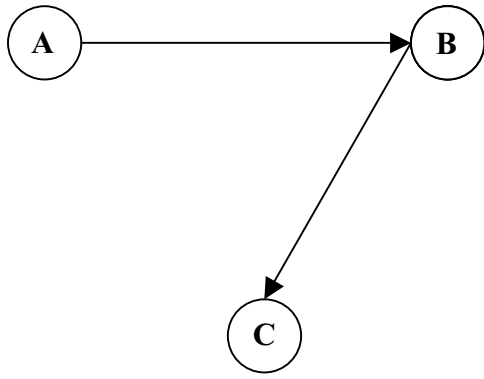
Figure 2: Reconstructed attractors from time series from Example 1. (a) Driving attractor; (b) linearly driven attractor; (c) nonlinearly driven attractor.

Figure 3: Extended Granger Causality Index (EGCI) as a function of the size δ of the neighborhood from Example 1. (a) Linear driving case; (b) nonlinear driving case.

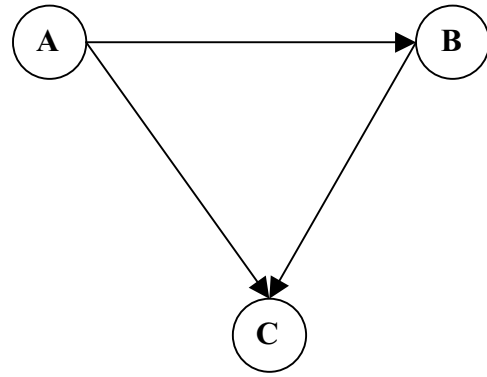
Figure 4: EGCI between two time series from Examples 2 and 3. (a) ODEs with a stable fixed point and different coupling strengths; (b) ODEs with chaotic behavior.

Figure 5: Simulating two patterns of interactions in Figure 1 with three coupled AR models (Example 4). (a) Pairwise analysis results; (b) Conditional causality analysis separates the two cases. Dotted line gives the Conditional Extended Granger Causality Index (CEGCI) for $c = 0.5$ and the solid line for $c = 0$.

Figure 6: Simulating two patterns of interactions in Figure 1 with three coupled chaotic 1d-maps (Example 4). (a) Pairwise analysis results, the two patterns of interaction are not distinguished; (b) CEGCI analysis is able to distinguish between the two different patterns. Dotted line gives the CEGCI for $c = 0.5$ and the solid line for $c = 0$.

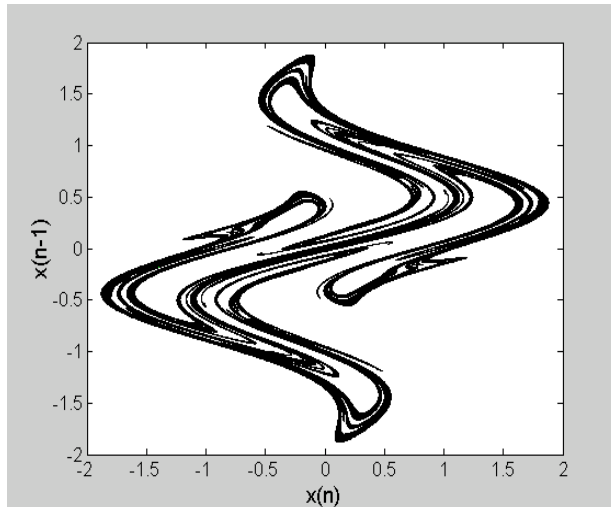


(a)

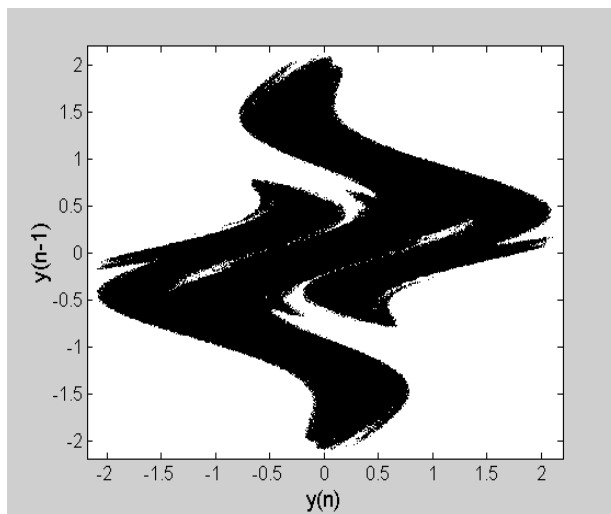


(b)

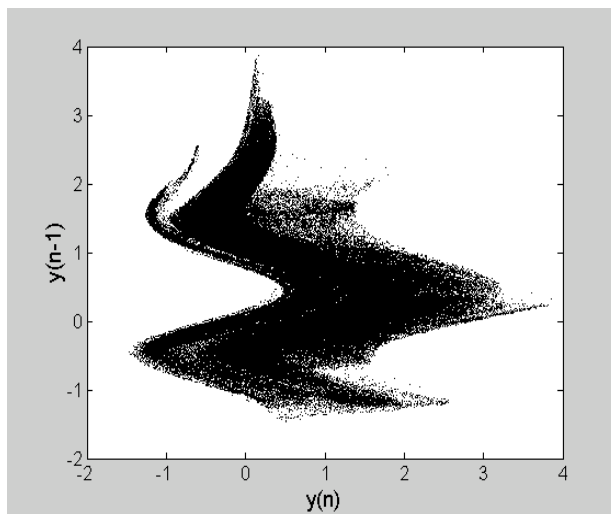
Fig. 1



(a)



(b)



(c)

Fig. 2

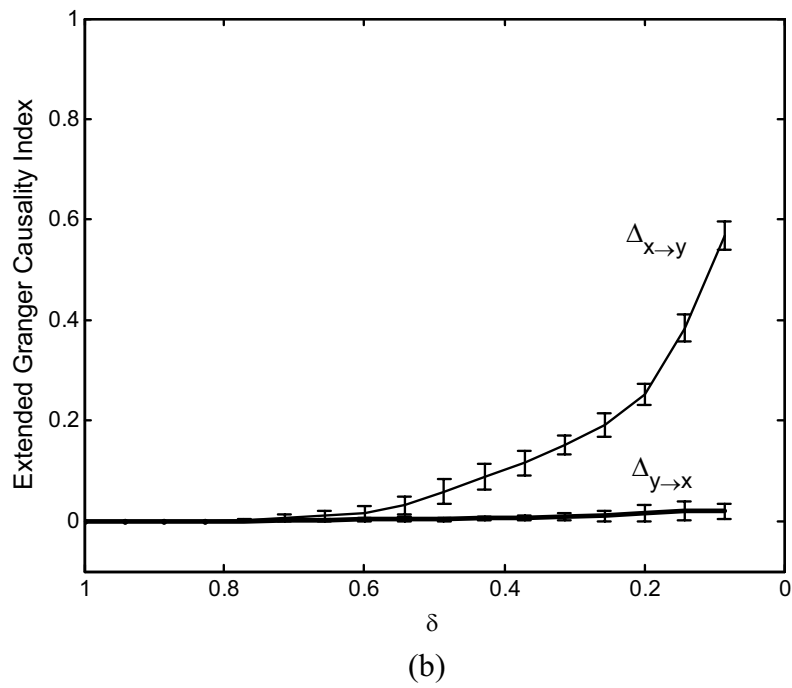
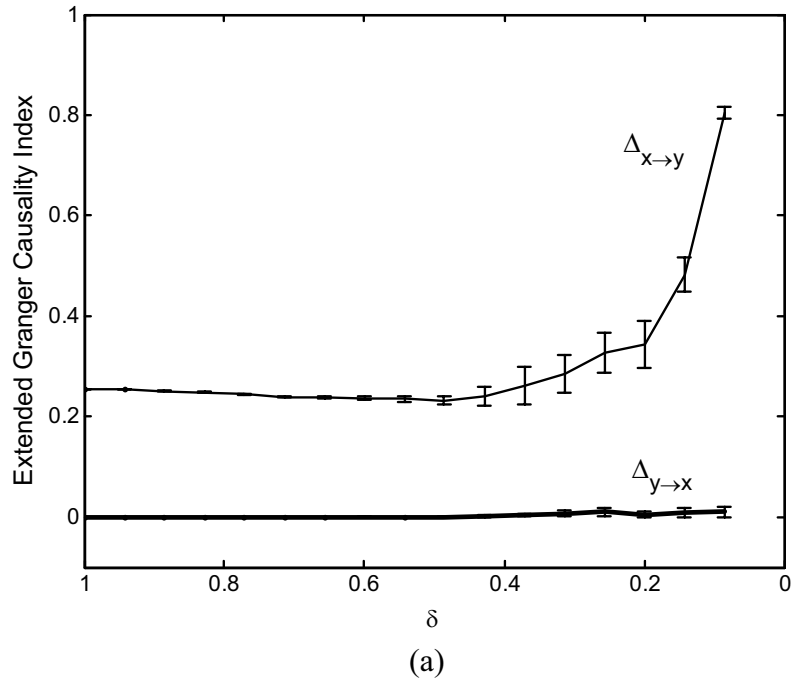


Fig. 3

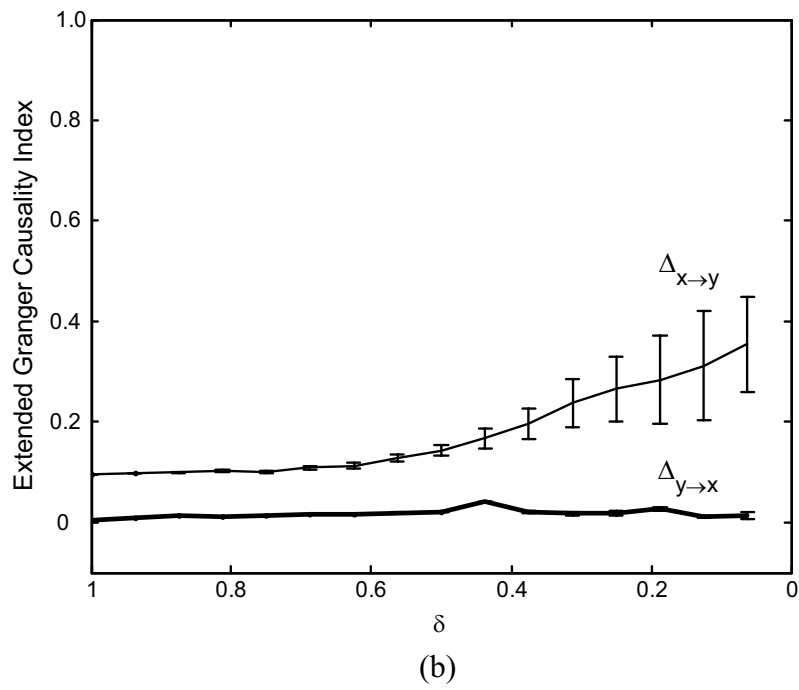
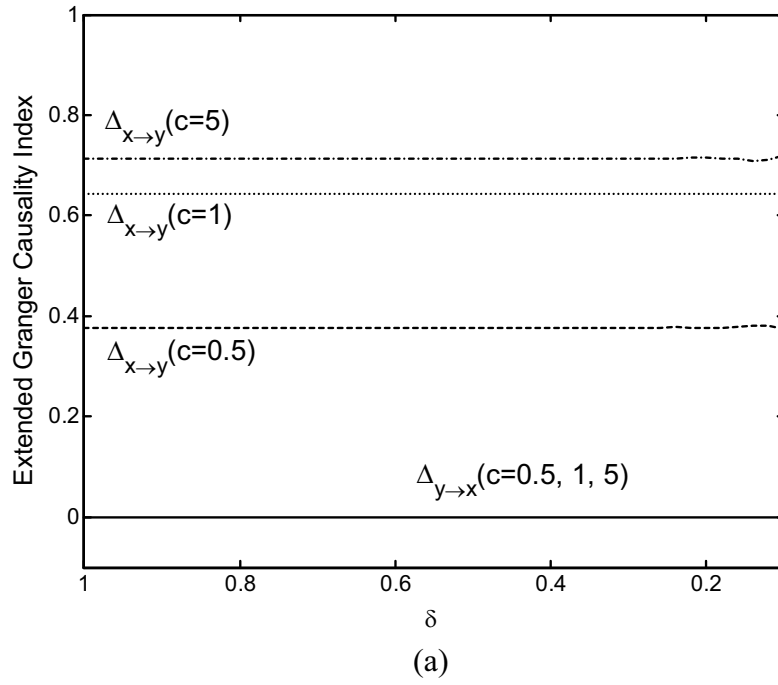


Fig. 4

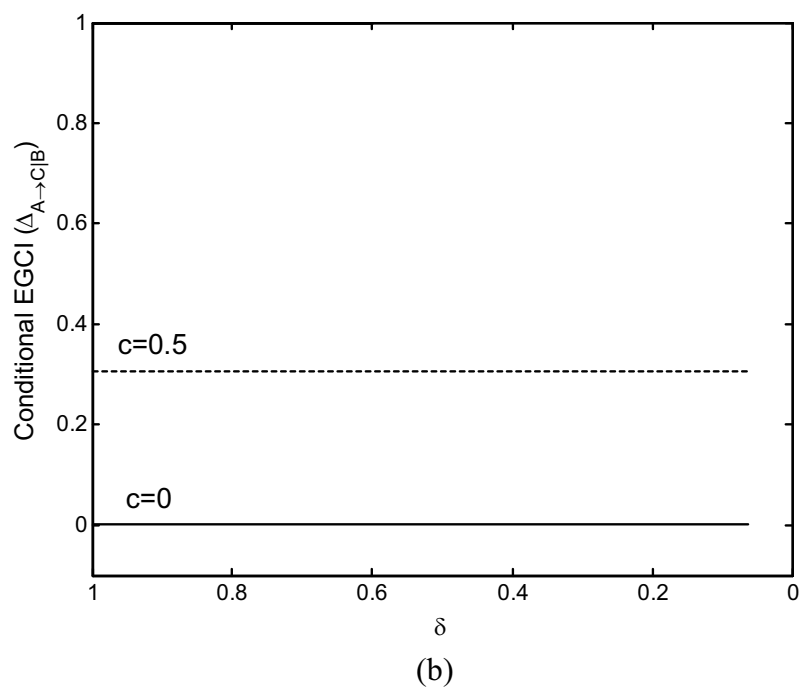
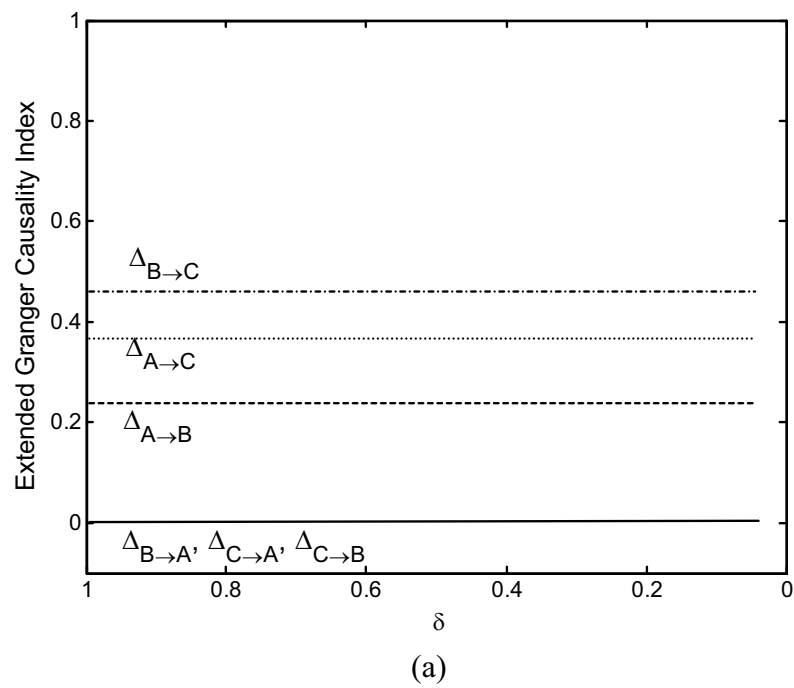
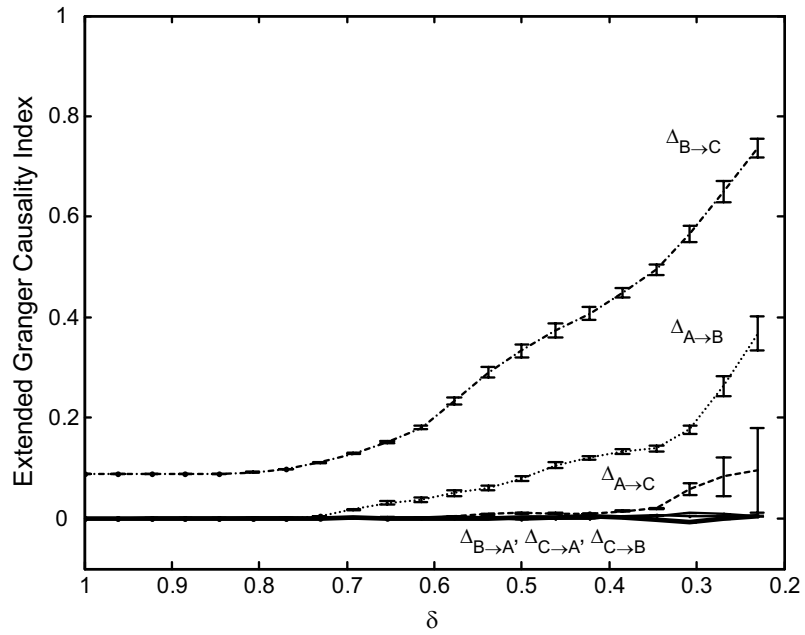
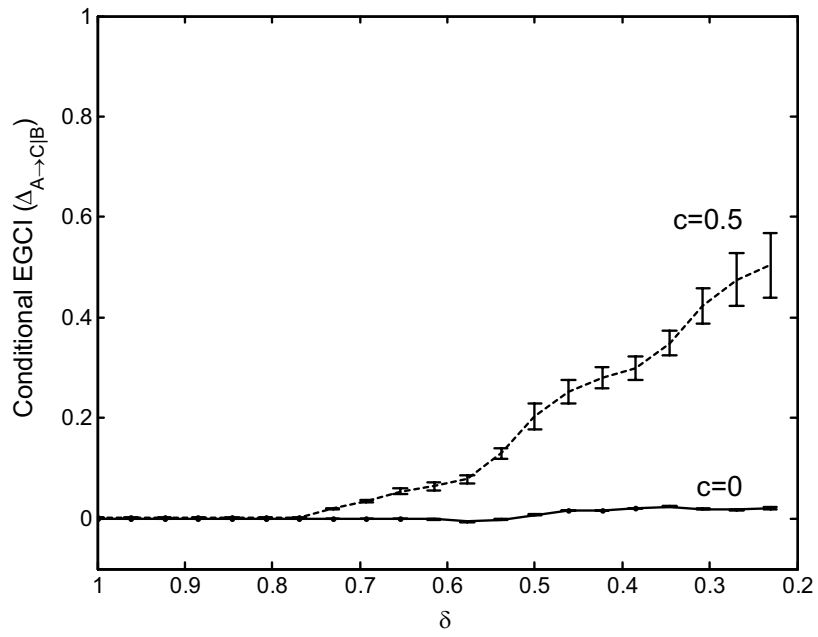


Fig. 5



(a)



(b)

Fig.6